OPEN

Deciphering the predictors of endometrial nonbenign lesions in asymptomatic postmenopausal women via explainable machine learning

Linlin Yang, PhD,[1,2,3] Chen Xu, MD,[1,2,3] Rongjia Su, PhD,[1,2,3] Xiaoyan Gao, MD,[1,2,3] Baoying Ye, PhD,[2,3,4] Yuan Liu, MD,[2,3,5] Jing Wang, PhD,[1,2,3] Yidan Chen, MD,[1,2,3] Qiong Fan, PhD,[1,2,3] Jiangjing Yuan, PhD,[1,2,3] Xiaojing Lu, PhD,[1,2,3] Dongjian Yang, MD,[6] Yuhong Li, BD,[1,2,3] and Yudong Wang, PhD[1,2,3]

Abstract

Objectives: Timely identification of endometrial nonbenign lesions led to improved outcomes, but there was a lack of effective predictive models for asymptomatic endometrial thickening. The aim of this study was to develop a strong machine learning (ML) model for assessing the risk of endometrial malignancy in asymptomatic patients after menopause.

Methods: This retrospective study was designed to collect data from 971 postmenopausal asymptomatic women with endometrial thickening. The bootstrap resampling method was used for model training, internal validation, and external validation. With 41 easily accessible characteristics, multifactor regression and least absolute shrinkage and selection operator regression were performed for feature selection. Nine ML algorithms were applied to build a model. To explain the final model and rank feature importance, the SHapley Additive exPlanation (SHAP) method was utilized. Meanwhile, a nomogram was developed to facilitate model interpretation.

Results: The comprehensive methodologies identified parity, Doppler flow signals, endometrial thickness, cancer antigen 125, and D-dimer as significant predictors. The logistic regression (LR) model demonstrated superior performance compared with other ML algorithms, achieving an accuracy of 88%, a sensitivity of 78%, a specificity of 98%, and an area under the receiver operating characteristic curve of 0.81. Furthermore, individualized predictions of endometrial malignancy were visualized

Received for publication August 23, 2025; accepted September 12, 2025.

From the [1]Department of Gynecological Oncology, The International Peace Maternity and Child Health Hospital, School of Medicine, Shanghai Jiao Tong University, Shanghai, China; [2]Department of Gynecological Oncology, The International Peace Maternity and Child Health Hospital, School of Medicine, Shanghai Jiao Tong University, Shanghai Municipal Key Clinical Specialty, Shanghai, China; [3]Department of Gynecological Oncology, The International Peace Maternity and Child Health Hospital, School of Medicine, Shanghai Jiao Tong University, Shanghai Key Laboratory of Embryo Original Disease, Shanghai, China; [4]Department of Ultrasonography, The International Peace Maternity and Child Health Hospital, School of Medicine, Shanghai Jiao Tong University, Shanghai, China; [5]Department of Pathology, The International Peace Maternity and Child Health Hospital, School of Medicine, Shanghai Jiao Tong University, Shanghai, China; and [6]Clinical Research Center, The International Peace Maternity and Child Health Hospital, School of Medicine, Shanghai Jiao Tong University, Shanghai, China.

Funding/Support: This study was supported by grants from the National Natural Science Foundation of China (Nos. 82304602, 82103029, and 82573837), the Shanghai Leading Talent Program of Eastern Talent Plan (LJ2024085), the Shanghai Science and Technology Committee (24Y22800300), the "Flagship" Department of Traditional Chinese and Western Medicine Synergy Project of National Administration of Traditional Chinese Medicine (No. ZXXTQJ-2024), the Collaborative Guidance Project of Traditional Chinese and Western Medicine in General Hospitals of Shanghai (No. ZXXT-202315), the Project of Outstanding Young Scientific Research Talents from The International Peace Maternity and Child Health Hospital (No. GFY6203), and Shanghai "Rising Stars of Medical Talents" Youth Development Program (Youth Medical Talents-Specialist Program (SHWSRS(2025)_071)).

Financial disclosure/Conflicts of interest: None reported.

L.Y., C.X., and R.S. contributed equally to this work.

Author contributions: Y.L. performed the data analyses and drafted the manuscript. X.C. and S.R. established the machine learning models. G.X., Y.B., L.Y., W.J., C.Y., F.Q., and Y.J. participated in data collection and processing. L.X. and Y.D. participated in the design of the study and coordination. L.Y. and W.Y. accessed and verified the data. All authors read and approved the final manuscript.

Data availability statement: All the data have been provided within the manuscript or supplementary information files.

Ethical approval and consent to participate: This study included human participants, and the research proposal and procedures were reviewed and approved by the International Peace Maternity and Child Health Hospital. Written informed consent was obtained from participating patients for the research use of the medical information.

Supplemental Digital Content is available for this article. Direct URL citations are provided in the HTML and PDF versions of this article on the journal's website, www.menopause.org.

Address correspondence to: Yudong Wang, PhD. E-mail: wangyudong@shsmu.edu.cn; Yuhong Li, BD. E-mail: 13022107898@163.com, Department of Gynecological Oncology, The International Peace Maternity and Child Health Hospital, School of Medicine, Shanghai Jiao Tong University, 1961 Huashan Road, Shanghai 200060, China.

eISSN: 1530-0374
DOI: 10.1097/GME.0000000000002699

through a force plot generated by SHAP analysis. A nomogram based on the LR model was subsequently constructed, showing area under the receiver operating characteristic curve values of 0.82, 0.82, and 0.81 for the training, internal validation, and external validation cohorts, respectively. The calibration curve demonstrated excellent consistency.

Conclusions: We developed an LR-based nomogram model and interpreted using the SHAP method, which provided visual insights for detecting endometrial nonbenign lesions in asymptomatic postmenopausal women. This approach would aid clinicians in providing individualized treatment and help avoid unnecessary invasive surgeries.

Key Words: Endometrial malignancy, Machine learning, Nomogram, Postmenopausal asymptomatic women, Shapley Additive exPlanations (SHAP).

(*Menopause* 2026;33:593–607)

Endometrial cancer (EC) was the most prevalent gynecologic malignancy in the United States with 66,200 new cases and 13,030 deaths in 2023.[1] The rising incidence of uterine corpus cancer was about 1% per year since the mid-2000s among women aged 50 years and older, and its mortality continued to increase by about 1% per year.[2] Majority of patients diagnosed with EC suffered from postmenopausal bleeding (PMB), and the probability of developing EC was 5%-10%.[3] Transvaginal ultrasound scan (TVUS) with endometrial thickness (ET) measurement was the first-line investigation mode for women with PMB, and when the value was >4 or 5 mm, endometrial biopsy with or without hysteroscopy was further suggested.[4,5] While over 15% of endometrial malignancies occurred in postmenopausal women without bleeding,[6] there was no consensus on the optimal ET threshold for endometrial sampling in asymptomatic postmenopausal individuals.[7-11] Moreover, interpretable comprehensive analytical models to identify endometrial atypical hyperplasia (AH) and carcinoma in asymptomatic postmenopausal women were extremely uncommon.

With the advancement and the wide availability of ultrasound, the number of asymptomatic women with incidentally thickened endometrium was sharply elevated.[12] The occurrence rate of the thickened endometrium in asymptomatic postmenopausal women has been reported to range from 10% to 17%.[13] In this population, the prevalences of AH and EC were 0.62% and 0.59%, respectively.[14] Thus, applying the cutoff of ET of 4-5 mm for symptomatic individuals to all asymptomatic women would inevitably expose many low-risk women to invasive procedures, leading to the overuse of health care resources and economic waste.[15] A standardized ET cutoff value for this population was urgently essential. In addition, it was reported that chronic inflammation and carcinogenesis were closely related, contributing to a relative thrombocytosis, neutrophilia, and lymphocytopenia within the tumor microenvironment.[16] Multiple inflammatory and coagulation biomarkers, specifically the neutrophil-to-lymphocyte ratio (NLR), platelet-to-lymphocyte ratio (PLR), and more recently, the monocyte-to-lymphocyte ratio (MLR) and fibrinogen-to-albumin ratio (FAR), had been demonstrated to exhibit significant associations with various types of malignancies[17-20]; serum gamma-glutamyltransferase (GGT) was supposed to regulate cellular processes like redox balance which was associated with etiology of cancer.[21] Although complete blood count, coagulation function, and serum oncologic indicators such as cancer antigen 125 (CA125) and human epididymis protein 4 (HE4) were feasible and convenient parameters that could often be tested before operation in most clinics, research on the significance of these markers in identifying endometrial malignancy was scarce. The medical nomogram utilized biological and clinical variables to graphically depict a statistical model, which generated the probability of a clinical event for a specific study cohort.[22] If incorporating these parameters into a nomogram model to develop a predictive tool for endometrial malignancy, it would be conducive to optimizing the therapeutic plans for postmenopausal patients.

To date, artificial intelligence has been extensively employed to detect the early warning predictors of many diseases.[23] Machine learning (ML) could handle complex interactions and nonlinear relationships, resulting in its increased use in clinical research, and has recently demonstrated favorable performance in predicting clinical outcomes, but it was limited by the difficulty of stating the direct interpretation, known as a so-called "black-box," and hence was not actionable.[24] To overcome these issues, the SHapley Additive exPlanation (SHAP) method was utilized.[25] Nevertheless, no researchers have yet focused on constructing a robust ML model specifically for postmenopausal elderly women with asymptomatic endometrial thickening, nor has the explainable SHAP approach been utilized to visualize individual variable predictions.

This study aimed to integrate clinical features, ultrasound findings, and hematological indicators to develop an interpretable ML model that could accurately predict endometrial precancerous and cancerous lesions in postmenopausal patients with asymptomatic thickened endometrium, thereby guiding surgical interventions and supporting clinical decision-making.

METHODS

Study population

Between January 2017 and August 2024, postmenopausal women who were detected with asymptomatic thickened endometrium by transvaginal sonography (TVUS) for hysteroscopy assessment at the International Peace Maternity and Child Health Hospital (Shanghai, China) (IPMCH) were retrospectively enrolled in this study. Participants fulfilled the following inclusion criteria: (1) postmenopausal patients who underwent hysteroscopy due to asymptomatic endometrial thickening (≥ 5 mm) in our hospital and obtained postoperative pathological

results, (2) patients who underwent ultrasound and blood biochemical examinations within 1 week before surgery in our hospital, and (3) patients whose clinical characteristics were complete and available. The exclusion criteria were as follows: (1) patients with natural menopause <12 months, (2) patients who had postmenopausal vaginal bleeding or discharge, (3) the last TVUS was not monitored within a week before hysteroscopy at this hospital by senior sonographer, (4) participants who had incomplete preoperative data, and (5) patients treated with anticoagulant or antiplatelet drugs such as aspirin and clopidogrel. Finally, of the 2,518 screened patients from IPMCH, 745 patients were eligible for inclusion in the present study. The patients were then randomly divided into two independent groups by R software according to the ratio of 7:3, of which 522 patients were in the training cohort and 223 were in the internal validation cohort. In addition, to investigate the performance of the nomogram model in predicting endometrial malignancy, an external data set consisting of 226 postmenopausal patients with asymptomatic endometrial thickening admitted to the Shanghai General Hospital for hysteroscopy examination from January 2021 to January 2022 was employed for the external validation. The inclusion and exclusion criteria were identical to those of the derivation cohort. This study was approved by the Institutional Ethics Committee of IPMCH hospital, and written informed consents were obtained from all participants. The patients' data were deidentified and reorganized in accordance with ethical standards.

Study indicators

The following clinicopathological variables were obtained: (1) demographic features, including age, duration of menopause, gravidity, parity, miscarriages, body mass index, hypertension, hyperlipidemia, diabetes, coronary heart disease, history of breast cancer, and use of tamoxifen. (2) The detection indexes by TVUS: Doppler flow signals, and ET. (3) Preoperative laboratory examination, including CA125, human epididymis 4 (HE4), GGT, white blood cells, neutrophils, lymphocytes, monocytes, platelet count, hematocrit, red cell distribution width, mean platelet volume, platelet distribution width, platelet-larger cell ratio, platelet thrombocytocrit, albumin, neutrophil count and lymphocyte count ratio (NLR), platelet count and lymphocyte count ratio (PLR), monocyte count and lymphocyte count ratio (MLR), fibrinogen and albumin ratio (FAR), prothrombin time, international normalized ratio, activated partial thromboplastin time, fibrinogen, thrombin time, D-dimer, fibrin degradation products. The values of body mass index, NLR, PLR, MLR, and FAR were calculated based on the corresponding preoperative values. All measurements were performed in strict accordance with the manufacturer's requirements. Transvaginal gray-scale and color Doppler ultrasound examination was performed by experienced sonographers using a standardized examination technique.[26] Moreover, to avoid overfitting, the least absolute shrinkage and selection operator (LASSO) was used to select and filtrate the independent risk factors.[23]

Model development and explanation

Multiple ML classification models were applied for comprehensive analysis after selecting characteristic factors from all independent variables. We constructed and tested nine supervised ML models by using their default hyperparameter settings in the Python Scikit-learn library: light gradient boosting machine (LightGBM), logistic regression (LR), random forest, extreme gradient boosting (XGBoost), support vector machine, gradient boosting machine (GBM), k-nearest neighbors, gaussian mixture model, and decision tree. The commonly used evaluation indexes, including the area under the receiver-operating-characteristic (ROC) curve (AUC), sensitivity, specificity, positive predictive value (PPV), negative predictive value (NPV), accuracy, and F1 score, were used to evaluate the reliability of these models[27]; we then screened out the optimal model.

The elucidation of the prediction model was accomplished by the SHAP method, which was a unified approach to rank the importance of input features and explicate the effects of features on the predicted results.[28] SHAP values, which possessed additivity and interpretability properties, represented the extent to which a prediction changes when a feature value was given, relative to the average prediction.[29] Of note, SHAP visually offered both global and local explanations of the model, and the latter could demonstrate a specific prediction for an individual patient by inputting the specific information.[30]

In addition, a combined nomogram model was developed using highly correlated indicators identified through LR analysis.[31] The accuracy of quantitative prediction was investigated by using AUC. The consistency between the predicted results and the actual results was explored by calibration curve and its clinical effectiveness was determined by using decision curve analysis (DCA).

Statistical analysis

Data analyses were conducted by using Python version 3.6.5 (https://www.python.org), SPSS Statistical Software Version 26.0 (https://www.ibm.com/spss), and R version 4.0.1 (https://www.R-project.org). Continuous data with skewed distributions were expressed as median with interquartile range and compared using the Mann-Whitney U test. Categorical variables were expressed as frequencies with percentages and compared using the χ^2 test or Fisher exact test. The receiver operating characteristic (ROC) curves were used to evaluate the predictive power of the model, and the optimal cutoff value was built by maximizing the Youden index. A bilateral P value <0.05 was considered statistically significant.

RESULTS

Patient characteristics

From January 2017 to August 2024, a total of 745 eligible postmenopausal women in our hospital who underwent hysteroscopy due to endometrial thickening detected by the TVUS examination were included in this

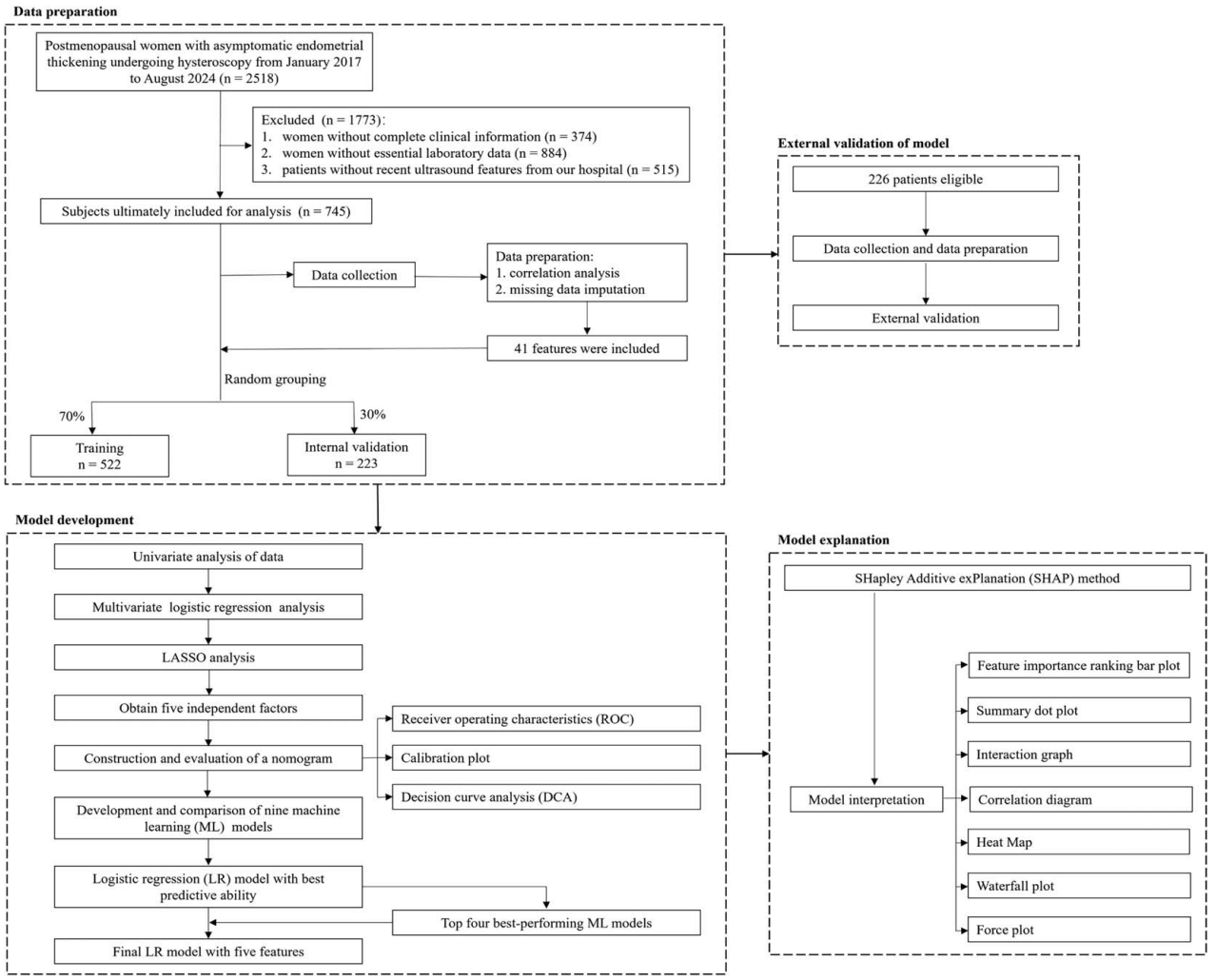

FIG. 1. Flow chart of the study design. LASSO, least absolute shrinkage and selection operator.

study; another 1773 cases who did not meet the inclusion criteria were excluded. These 745 candidates were randomly allocated into a training set (n = 552) and an internal validation set (n = 223) at a 7:3 ratio. In addition, the external cohort consisting of 226 patients was utilized as the external validation set. Details of the flowchart are displayed in Figure 1.

The pathological results of hysteroscopic diagnostic curettage from thickened endometrium were listed in Table 1 and Supplementary Figure 1, Supplemental Digital Content 1, http://links.lww.com/MENO/B463. Among them, 648 patients (87.0%) were identified as having benign pathological results, including 457 (61.3%) with endometrial polyps, 27 (3.6%) with submucosal fibroids, 18 (2.4%) with endometritis, 46 (6.2%) with atrophic endometrium, 69 (9.3%) with proliferative endometrium, and 31 (4.2%) with endometrial hyperplasia without atypia. These were defined as a benign group. In addition, there were 28 cases (3.8%) of AH and 69 cases (9.3%) of endometrial carcinoma (EC), which were classified as the malignant group. In addition, we further tracked the results of the subsequent staging surgeries. Among 28 women diagnosed with AH, 2 patients (7.1%) were upstaged to endometrioid carcinoma. Of the 69 women with EC, 61 cases underwent staging surgery in our hospital, 52 individuals (88.1%) were classified as stage I, 1 patient (1.7%) as stage II, and 6 (10.2%) as stage III. Regarding pathological types, there were 53 cases (86.9%) of endometrioid adenocarcinoma and 8 cases (13.1%) of non-

TABLE 1. Pathologic outcomes in postmenopausal asymptomatic women with thickened endometrium

Type	Overall (n = 745) (%)
Normal endometrium	648 (87.0)
Endometrial polyps	457 (61.3)
Submucosal fibroids	27 (3.6)
Endometritis	18 (2.4)
Atrophic endometrium	46 (6.2)
Proliferative phase endometrium	69 (9.3)
Endometrial hyperplasia without atypia	31 (4.2)
Atypical hyperplasia	28 (3.8)
Endometrial cancer	69 (9.3)

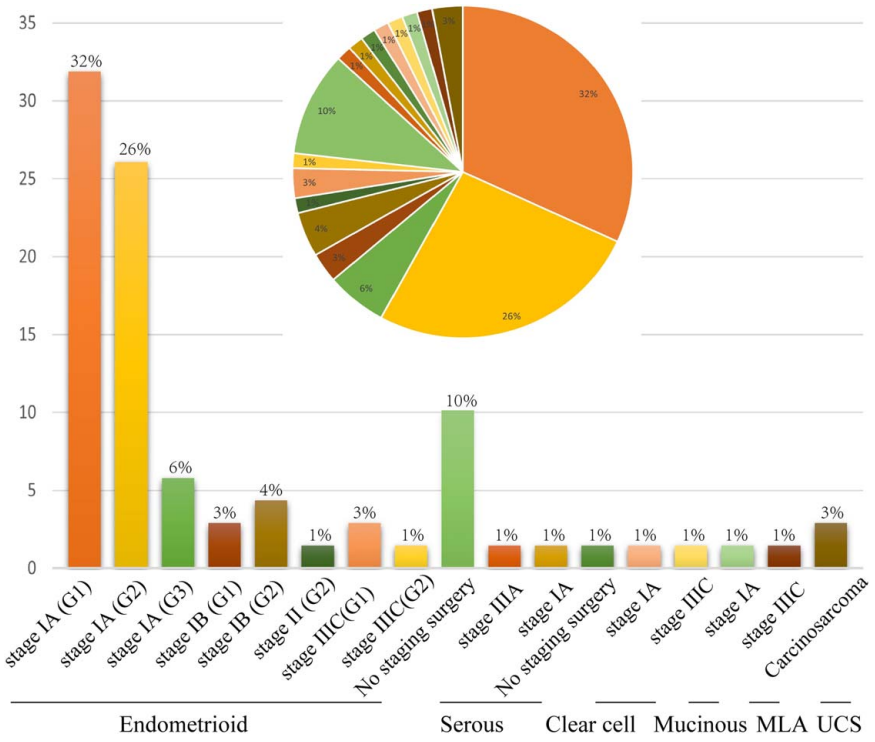

FIG. 2. Presentation of pathological outcomes among EC patients. EC, endometrial carcinoma; MLA, mesonephric-like adenocarcinoma; UCS, uterine carcinosarcoma.

endometrioid carcinoma (2 cases of serous carcinoma, 2 cases of clear cell carcinoma, 1 case of mucinous carcinoma, 1 case of mesonephric-like adenocarcinoma, and 2 cases of carcinosarcoma). The pathological outcomes were summarized in Figure 2, Supplementary Table 1, Supplemental Digital Content 1, http://links.lww.com/MENO/B463, and Supplementary Figure 2, Supplemental Digital Content 1, http://links.lww.com/MENO/B463. Subsequently, we attached importance to the distribution of ET in 745 participants who had undergone transvaginal ultrasonography (Supplementary Fig. 3A, Supplemental Digital Content 1, http://links.lww.com/MENO/B463 and Supplementary Table 2, Supplemental Digital Content 1, http://links.lww.com/MENO/B463). It was noted that the percentage of endometrial carcinoma and precancerous lesions increased in parallel with the thickening of the endometrium (Supplementary Fig. 3B, Supplemental Digital Content 1, http://links.lww.com/MENO/B463). ET in different histopathological categories was also shown in Supplementary Figure 4, Supplemental Digital Content 1, http://links.lww.com/MENO/B463. In the training cohort, the mean ET was found to be significantly greater in patients with AH/EC (10.75 ± 4.86) than in those with endometrial polyps (8.16 ± 3.22, $P = 0.000$), submucosal fibroids (6.60 ± 1.10, $P = 0.000$), endometritis (6.01 ± 1.10, $P = 0.000$), endometrial atrophy (7.03 ± 1.90, $P = 0.000$), and proliferative endometrium (8.20 ± 2.93, $P = 0.001$). The same finding was observed in the validation set (Supplementary Table 3, Supplemental Digital Content 1, http://links.lww.com/MENO/B463). Specifically, in both the training and validation sets, the ET value was significantly higher in the malignant group than in the benign group: the respective comparisons were 10.75 ± 4.86 versus 8.00 ± 3.04 ($P < 0.001$) for the training set and 11.49 ± 5.09 versus 7.83 ± 2.94 ($P < 0.000$) for the validation set. Further, ROC analysis was used to explore the cutoff value of ET for predicting endometrial malignancy in this asymptomatic cohort (Supplementary Fig. 5, Supplemental Digital Content 1, http://links.lww.com/MENO/B463). The result indicated that the diagnostic threshold for ET was 8.15 mm with an AUC of 0.716 (95% CI: 0.661-0.743), a sensitivity of 75.0%, and a specificity of 68.0%.

Comparison of baseline characteristics

To propose a more systematic method for identifying malignancy in postmenopausal patients with thickened endometrium, clinical and ultrasonic features combined with preoperative blood routine, coagulation function, and tumor indicators were comprehensively analyzed. After randomization grouping, the training and validation sets exhibited similar parameters ($P > 0.05$) (Table 2). In the training cohort, the history of parity, positive Doppler flow signals, ET by ultrasound imaging, the concentration of CA125, red cell distribution width, and D-dimer by hematological tests between the benign and malignant groups were statistically significant ($P < 0.05$). The content of HE4 in the malignant group was higher than that in the benign group, but the difference was not significant ($P = 0.062$). As the levels of inflammatory response

TABLE 2. Baseline characteristics in training and validation cohorts

Variables	No. of patients Overall (N = 745) (%)	Training set (n = 522) (%)	Validation set (n = 223) (%)	*P*
Age (y)	61.93 ± 6.58	62.05 ± 6.57	61.63 ± 6.61	0.450
Duration of menopause (y)	10.00 (5.00, 15.00)	10.00 (5.00, 15.00)	10.00 (5.00, 15.00)	0.727
Gravidity	2.00 (2.00, 3.00)	2.00 (2.00, 3.00)	2.00 (2.00, 3.00)	0.802
Parity	1.00 (1.00, 1.00)	1.00 (1.00, 1.00)	1.00 (1.00, 1.00)	0.252
Miscarriages	1.00 (0.00, 2.00)	1.00 (0.00, 2.0)	1.00 (0.00, 2.00)	0.390
BMI (kg/m^2)	24.57 ± 3.44	24.58 ± 3.48	24.52 ± 3.34	0.900
Hypertension, n (%)				
No	449 (60.30)	317 (60.70)	132 (59.20)	0.695
Yes	296 (39.70)	205 (39.30)	91 (40.80)	
Hyperlipidemia, n (%)				
No	722 (96.90)	507 (97.10)	215 (96.40)	0.606
Yes	23 (3.10)	15 (2.90)	8 (3.60)	
Diabetes, n (%)				
No	681 (91.40)	477 (91.40)	204 (91.50)	0.964
Yes	64 (8.60)	45 (8.60)	19 (8.50)	
Coronary heart disease, n (%)				
No	722 (96.90)	505 (96.70)	217 (97.40)	0.682
Yes	23 (3.10)	17 (3.30)	6 (2.70)	
History of breast cancer, n (%)				
No	706 (94.80)	496 (95.00)	210 (94.20)	0.634
Yes	39 (5.20)	26 (5.00)	13 (5.80)	
Use of tamoxifen, n (%)				
No	715 (96.00)	503 (96.40)	212 (95.10)	0.411
Yes	30 (4.00)	19 (3.60)	11 (4.90)	
Positive Doppler flow signals, n (%)				
No	718 (96.40)	502 (96.20)	216 (96.90)	0.643
Yes	27 (3.60)	20 (3.80)	7 (3.10)	
Endometrial thickness (mm)	8.34 ± 3.47	8.36 ± 3.46	8.30 ± 3.50	0.571
CA125 (U/mL)	11.60 (8.90, 15.20)	11.40 (9.00, 15.20)	12.20 (8.80, 15.30)	0.518
HE4 (pmol/L)	56.60 (46.40, 63.10)	53.40 (46.40, 62.80)	54.50 (46.30, 65.00)	0.513
GGT (IU/L)	21.00 (16.00, 32.00)	22.00 (16.00, 33.80)	20.00 (15.50, 31.50)	0.112
WBC ($\times 10^9$/L)	6.00 (5.10, 7.10)	6.00 (5.10, 7.20)	6.00 (5.10, 7.00)	0.919
Neutrophils ($\times 10^9$/L)	3.60 (3.00, 4.60)	3.60 (3.00, 4.70)	3.60 (2.90, 4.30)	0.537
Lymphocytes ($\times 10^9$/L)	1.80 (1.40, 2.20)	1.80 (1.40, 2.10)	1.80 (1.40, 2.20)	0.757
Monocytes ($\times 10^9$/L)	0.40 (0.30, 0.50)	0.40 (0.30, 0.50)	0.40 (0.30, 0.50)	0.506
PLT ($\times 10^9$/L)	229.00 (195.00, 266.00)	226.00 (194.00, 265.20)	234.00 (196.00, 272.00)	0.414
HCT (%)	39.70 (38.10, 41.80)	39.70 (38.10, 41.80)	39.80 (37.80, 42.00)	0.739
MCV (fL)	91.20 (88.60, 93.80)	91.30 (88.70, 93.70)	90.80 (88.30, 94.00)	0.493
RDW (%)	12.50 (12.10, 12.90)	12.50 (12.10, 12.90)	12.50 (12.20, 12.90)	0.346
MPV (fL)	10.40 (9.90, 11.10)	10.40 (9.90, 11.10)	10.40 (9.80, 11.10)	0.519
PDW (fL)	12.00 (10.80, 13.30)	12.00 (10.80, 13.30)	11.90 (10.70, 13.60)	0.908
P-LCR (%)	28.30 (23.90, 33.90)	28.20 (24.00, 33.80)	28.40 (23.10, 34.00)	0.844
PCT (%)	0.20 (0.20, 0.30)	0.20 (0.20, 0.30)	0.20 (0.20, 0.30)	0.414
Albumin (g/dL)	45.10 (42.40, 47.60)	45.30 (42.80, 47.40)	44.80 (42.20, 48.70)	0.905
NLR	2.10 (1.50, 2.70)	2.10 (1.60, 2.80)	2.10 (1.50, 2.60)	0.350
PLR	130.50 (103.10, 164.70)	130.50 (102.80, 164.20)	129.80 (103.80, 167.10)	0.691
MLR	0.22 (0.17, 0.28)	0.21 (0.18, 0.28)	0.21 (0.17, 0.27)	0.213
FAR	0.07 (0.06, 0.08)	0.06 (0.06, 0.07)	0.06 (0.05, 0.07)	0.447
PT (s)	12.60 (12.20, 13.00)	12.60 (12.20, 13.00)	12.60 (12.30, 13.00)	0.402
INR	0.90 (0.90, 1.00)	0.90 (0.09, 1.00)	0.90 (0.90, 1.00)	0.310
APTT (s)	34.70 (32.20, 37.20)	34.70 (32.20, 37.20)	34.90 (32.30, 37.30)	0.456
Fibrinogen (g/L)	3.00 (2.70, 3.30)	3.00 (2.60, 3.40)	3.00 (2.70, 3.30)	0.687
TT (s)	16.90 (16.30, 17.50)	16.90 (16.30, 17.50)	16.90 (16.40, 17.50)	0.463
D-dimer (mg/L)	0.30 (0.20, 0.40)	0.30 (0.20, 0.40)	0.30 (0.20, 0.40)	0.102
FDP (mg/L)	1.60 (1.20, 2.00)	1.60 (1.20, 2.00)	1.60 (1.10, 2.00)	0.579

APTT, activated partial thromboplastin time; BMI, body mass index; CA125, cancer antigen 125; FAR, fibrinogen and albumin ratio; FDP, fibrin degradation products; GGT, gamma-glutamyltransferase; HCT, hematocrit; HE4, human epididymis 4; INR, international normalized ratio; IQR, interquartile range; MCV, mean corpuscular volume; MLR, monocyte count and lymphocyte count ratio; MPV, mean platelet volume; NLR, neutrophil count and lymphocyte count ratio; P-LCR, platelet-larger cell ratio; PCT, platelet thrombocytocrit; PDW, platelet distribution width; PLR, platelet count and lymphocyte count ratio; PLT, platelet count; PT, prothrombin time; RDW, red cell distribution width; TT, thrombin time; WBC, white blood cells.

TABLE 3. Comparison of demographic, ultrasonographic, and hematological parameters in training and validation sets

	Training set (n = 522)			Validation set (n = 223)		
Variables	**Benign group (n = 454)**	**Malignant group (n = 68)**	***P***	**Benign group (n = 194)**	**Malignant group (n = 29)**	***P***
Age (y)	62.00 (57.00, 67.00)	61.00 (56.00, 67.00)	0.463	62.00 (57.00, 66.00)	60.00 (53.50, 64.50)	0.058
Duration of menopause (y)	10.00 (5.00, 15.00)	10.00 (5.00, 17.00)	0.954	9.00 (6.50, 10.00)	10.00 (5.50, 15.00)	0.050
Gravidity	2.0 (2.0, 3.0)	2.0 (2.0, 3.0)	1.000	2.0 (2.0, 3.0)	2.0 (1.0, 3.0)	0.068
Parity	1.0 (2.0, 1.0)	1.0 (1.0, 1.0)	0.048	1.0 (2.0, 1.0)	1.0 (1.0, 1.0)	0.049
Miscarriages	1.0 (0.0, 2.0)	1.0 (1.0, 2.0)	0.054	1.0 (1.0, 2.0)	1.0 (0.0, 2.0)	0.273
BMI (kg/m^2)	24.10 (22.00, 26.60)	24.75 (21.90, 26.90)	0.754	24.15 (22.30, 26.33)	24.70 (21.80, 28.25)	0.136
Hypertension, n (%)						
No	275 (60.6)	42 (61.8)	0.851	114 (58.8)	18 (62.1)	0.735
Yes	179 (39.4)	26 (38.2)		80 (41.2)	11 (37.9)	
Hyperlipidemia, n (%)						
No	441 (97.1)	66 (97.1)	1.000	187 (96.4)	28 (96.6)	1.000
Yes	13 (2.9)	2 (2.9)		7 (3.6)	1 (3.4)	
Diabetes, n (%)						
No	418 (92.1)	59 (86.8)	0.146	176 (90.7)	28 (96.6)	0.480
Yes	36 (7.9)	9 (13.2)		18 (9.3)	1 (3.4)	
Coronary heart disease, n (%)						
No	440 (96.9)	65 (95.6)	0.475	189 (97.4)	28 (96.6)	0.571
Yes	14 (3.1)	3 (4.4)		5 (2.6)	1 (3.4)	
History of breast cancer, n (%)						
No	430 (94.7)	66 (97.1)	0.558	182 (93.8)	28 (96.6)	1.000
Yes	24 (5.3)	2 (2.9)		12 (6.2)	1 (3.4)	
Use of tamoxifen, n (%)						
No	436 (96.0)	67 (98.5)	0.492	184 (94.8)	28 (96.6)	1.000
Yes	18 (4.0)	1 (1.5)		10 (5.2)	1 (3.4)	
Positive Doppler flow signals, n (%)						
No	445 (98.0)	57 (83.8)	0.001	190 (97.9)	26 (89.7)	0.001
Yes	9 (2.0)	11 (16.2)		4 (2.1)	3 (10.3)	
Endometrial thickness (mm)	8.00 ± 3.04	10.75 ± 4.86	< 0.001	7.83 ± 2.94	11.49 ± 5.01	< 0.000
CA125 (U/mL)	11.00 (8.50, 14.00)	15.20 (11.0, 22.75)	< 0.001	11.70 (8.65, 14.88)	14.20 (10.85, 20.26)	0.006
HE4 (pmol/L)	52.45 (45.25, 61.20)	55.90 (48.80, 68.70)	0.062	55.00 (46.10, 65.36)	53.80 (46.38, 64.71)	0.364
GGT (IU/L)	22.00 (16.00, 33.50)	22.00 (15.00, 34.00)	0.678	20.00 (16.00, 28.00)	19.00 (14.00, 35.00)	0.526
WBC ($\times 10^9$/L)	6.00 (5.10, 7.24)	6.00 (4.88, 7.46)	0.998	6.00 (5.20, 7.00)	6.20 (5.00, 7.50)	0.989
Neutrophils ($\times 10^9$/L)	3.50 (2.91, 4.63)	3.91 (2.91, 4.77)	0.549	3.60 (2.90, 4.30)	3.50 (2.90, 5.00)	0.891
Lymphocytes ($\times 10^9$/L)	1.80 (1.40, 2.17)	1.70 (1.37, 2.03)	0.477	1.80 (1.40, 2.20)	1.60 (1.20, 1.90)	0.071
Monocytes ($\times 10^9$/L)	0.40 (0.30, 0.50)	0.40 (0.30, 0.50)	0.642	0.40 (0.30, 0.50)	0.40 (0.30, 0.50)	0.830
PLT ($\times 10^9$/L)	226.00 (194.00, 265.00)	233.50 (202.80, 265.80)	0.625	227.00 (197.50, 260.00)	235.00 (195.00, 273.00)	0.699
HCT (%)	39.60 (38.10, 41.70)	40.10 (37.40, 42.00)	0.502	39.80 (38.00, 42.00)	39.60 (37.30, 41.70)	0.662
MCV (fL)	91.36 (88.17, 93.62)	92.26 (88.70, 93.97)	0.407	91.00 (88.50, 94.10)	90.10 (87.00, 93.20)	0.381
RDW (%)	12.50 (12.10, 12.90)	12.62 (12.33, 13.17)	0.037	12.40 (12.10, 12.80)	12.60 (12.30, 13.20)	0.028
MPV (fL)	10.40 (9.90, 11.10)	10.60 (10.00 11.20)	0.350	10.50 (9.80, 11.10)	10.30 (9.80, 11.20)	0.648
PDW (fL)	11.90 (10.80, 13.20)	12.20 (11.50, 13.60)	0.050	12.00 (10.60, 13.50)	11.90 (11.00, 13.80)	0.966
P-LCR (%)	28.10 (23.90, 33.80)	28.90 (25.90, 33.90)	0.252	28.90 (23.00, 34.00)	28.60 (23.80, 35.00)	0.736
PCT (%)	0.20 (0.20, 0.30)	0.20 (0.20, 0.30)	0.573	0.20 (0.20, 0.30)	0.20 (0.20, 0.30)	0.521
Albumin (g/dL)	45.41 (42.63, 47.64)	44.70 (43.00, 47.00)	0.672	45.90 (42.60, 48.80)	43.50 (40.30, 47.90)	0.192
NLR	2.00 (1.50, 2.78)	2.30 (1.70, 2.70)	0.396	2.00 (1.50, 2.60)	2.30 (1.70, 3.10)	0.173
PLR	129.70 (100.70, 164.90)	133.50 (115.10, 156.40)	0.450	129.70 (103.80, 163.70)	133.10 (106.10, 198.20)	0.252
MLR	0.21 (0.18, 0.28)	0.23 (0.18, 0.28)	0.461	0.20 (0.17, 0.27)	0.25 (0.17, 0.33)	0.155
FAR	0.07 (0.06, 0.08)	0.07 (0.06, 0.07)	0.731	0.06 (0.06, 0.07)	0.07 (0.05, 0.10)	0.389
PT (s)	12.50 (12.20, 12.90)	12.70 (12.30, 13.00)	0.218	12.60 (12.30, 12.90)	12.60 (12.10, 13.00)	0.914
INR	0.90 (0.90, 1.00)	0.90 (0.90, 1.00)	0.260	0.90 (0.90, 1.00)	0.90 (0.90, 1.00)	0.910
APTT (s)	34.70 (32.20, 37.40)	34.60 (31.60, 36.20)	0.284	34.90 (32.40, 37.30)	34.70 (32.20, 37.20)	0.885
Fibrinogen (g/L)	3.00 (2.60, 3.40)	3.10 (2.70, 3.40)	0.495	3.00 (2.70, 3.30)	3.10 (2.80, 3.70)	0.247
TT (s)	16.80 (16.30, 17.50)	17.00 (16.30, 17.90)	0.220	16.90 (16.40, 17.40)	17.00 (16.30, 18.00)	0.319
D-dimer (mg/L)	0.30 (0.20, 0.40)	0.40 (0.20, 0.70)	0.004	0.30 (0.20, 0.40)	0.40 (0.20, 0.50)	0.038
FDP (mg/L)	1.60 (1.20, 2.00)	1.60 (0.90, 2.10)	0.512	1.60 (1.10, 2.10)	1.40 (0.80, 1.70)	0.195

APTT, activated partial thromboplastin time; BMI, body mass index; CA125, cancer antigen 125; FAR, fibrinogen and albumin ratio; FDP, fibrin degradation products; GGT, gamma-glutamyltransferase; HCT, hematocrit; HE4, human epididymis 4; INR, international normalized ratio; IQR, interquartile range; MCV, mean corpuscular volume; MLR, monocyte count and lymphocyte count ratio; MPV, mean platelet volume; NLR, neutrophil count and lymphocyte count ratio; P-LCR, platelet-larger cell ratio; PCT, platelet thrombocytocrit; PDW, platelet distribution width; PLR, platelet count and lymphocyte count ratio; PLT, platelet count; PT, prothrombin time; RDW, red cell distribution width; TT, thrombin time; WBC, white blood cells.

TABLE 4. Multivariate logistic analysis to identify independent factors for endometrial malignancy

Variables	Odds ratio (95% CI)	*P*
Parity	0.299 (0.149-0.600)	< 0.001
Endometrial thickness (mm)	1.670 (1.389-2.356)	< 0.001
Positive Doppler flow signals	8.281 (2.267-30.253)	0.001
CA125 (U/mL)	1.429 (1.104-1.754)	0.021
RDW (%)	1.002 (0.821-1.223)	0.982
D-dimer (mg/L)	3.239 (1.535-6.835)	0.002

CA125, cancer antigen 125; RDW, red cell distribution width.

biomarker and coagulation had been associated with adverse clinical outcomes in endometrial tissues,[20,32,33] the preoperative NLR, PLR, MLR, and FAR ratios were also analyzed. The exploration revealed that neutrophil counts, platelet counts, and the ratios of NLR, PLR, and MLR were elevated in malignancies, but the results were not statistically significant. Although increased serum GGT was considered an independent risk factor of EC in Korea,[21] there were no significant differences in serum GGT level between the malignant and benign groups (Table 3). Subsequently, the factors with statistical difference were further selected for multivariate LR analysis, which indicated that parity, Doppler flow signals, ET, CA125, and D-dimer were independent contributors to the development of malignancy (Table 4 and Fig. 3). Then, the prediction equation was established as follows: the probability of malignancy = −1.208 × parity + 2.114 × blood signals + 0.157 × ET + 0.029 × CA125 + 1.175 × D-dimer − 2.495.

Screening of characteristic factors by LASSO analysis

LASSO regression analysis could compress variable coefficients to prevent overfitting and solve the problems of severe collinearity,[34] so LASSO was conducted on the total 41 variables with presence of malignancy as the dependent variable. It was worth noting that (lambda with minimum mean square error = 0.015) 41 variables were reduced to 11, including PLR, albumin, neutrophils, D-dimer, HE4, blood signals, ET, age, parity, use of tamoxifen, and CA125 (Fig. 4A, B). To further reduce the impact of confounding factors, the above 11 factors were intersected with the 5 independent variables by multivariate LR.[35] Finally, D-dimer, blood signals, ET, parity, and CA125 were screened out as characteristic factors.

Comprehensive analysis of classified multi-ML models

The selected features were utilized to generate nine ML models to predict the occurrence of endometrial malignancy. Among the nine models, LR model (AUC = 0.810) had the best predictive effect for endometrial malignancy with a sensitivity of 0.78, a specificity of 0.98, a PPV of 0.56, an NPV of 0.89, an accuracy of 0.88, and an F1 score of 0.59, followed by random forest model (AUC = 0.800), LightGBM model (AUC = 0.800), and XGBoost model (AUC = 0.780). The discriminative performances of these models are summarized in Table 5, and the ROC curves for the top four best-performing ML models are presented in Figure 5. Comprehensive analysis demonstrated that the LR model could be considered as the superior model.

The SHAP to model interpretation

To visually explicate the selected variables, we used SHAP to illustrate how these variables predicted the formation of EC in the model.[30] Figure 6A showed the ranking of five risk factors evaluated by the average absolute SHAP value, with the *x*-axis SHAP value exhibiting the importance of the forecast model. Ranked by mean absolute SHAP values from highest to lowest, the elements were listed as follows: CA125, ET, D-dimer, parity, and blood signal. The SHAP summary plot showed the impact of each feature on the prediction model (Fig. 6B). In each line, the attributions of all individuals to the results were plotted with different colored dots; the red dots represented high-risk values and blue dots denoted low-risk values. Based on the prediction model, a higher SHAP value of a feature indicated a greater likelihood of malignancy. Thus, reduced parity, positive blood flow signals, thickened endometrium, increased CA125, and D-dimer were associated with a higher SHAP value, indicating a higher likelihood of EC in postmenopausal asymptomatic patients. Figure 6C, D shows the summary plot of interaction values, which were obtained by decomposing the SHAP values of all features. A SHAP value plot, a type of heat map, was used to interpret the output of the ML model, which visually displayed how the

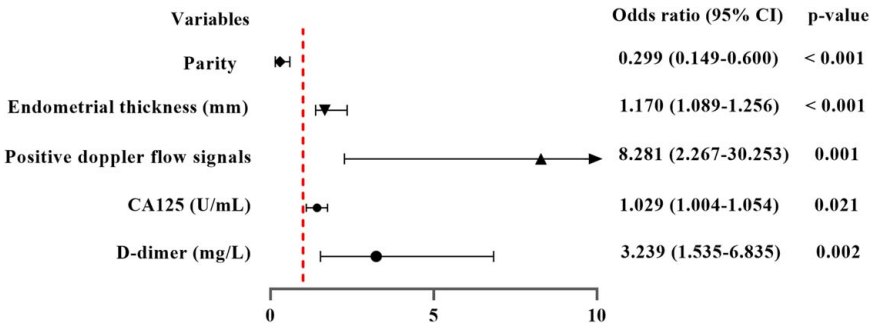

FIG. 3. The results of the multivariate logistic analysis are shown by the forest map.

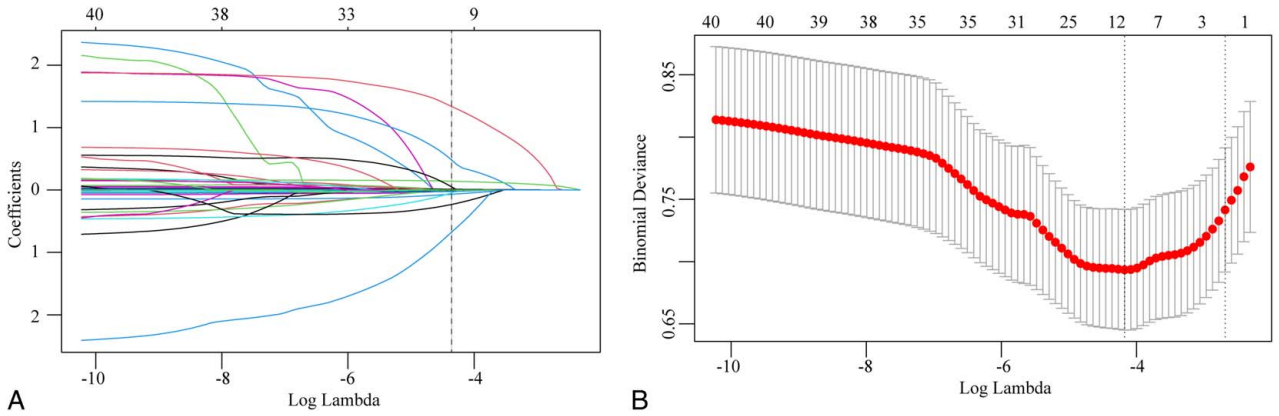

FIG. 4. LASSO regression analysis was used to select characteristic features. (**A**) The use of 10-fold cross-validation to draw vertical lines at selected values, where the optimal lambda could produce nonzero coefficients. (**B**) In the LASSO model, the profiles of 41 texture features were drawn from the log (λ) sequence. Vertical dotted lines were drawn at the minimum mean square error (λ = 0.015) and the standard error of the minimum distance (λ = 0.068). LASSO, least absolute shrinkage and selection operator.

five features affected model predictions. The plot visualized feature importance using a color scale, with each row representing a distinct feature and each column corresponding to an individual instance. The color intensity was correlated with the SHAP value, and red indicated a high positive influence on the model's output prediction, while blue indicated a negative impact (Fig. 6E). Furthermore, local explanation could display how a certain prediction was made for a specific case by incorporating the individualized data. Figure 6F shows a patient who did not develop EC with a thickened endometrium. It represented this patient toward the "EC" class with a probability of 4.6%, according to the prediction model. Furthermore, we presented two additional typical examples to display the interpretability of the model (Fig. 6G and Supplementary Fig. 6, Supplemental Digital Content 1, http://links.lww.com/MENO/B463). The color stood for the contributions of each feature, with red being positive and blue being negative, and the length of the color bar represented the contribution strength. For one patient, who was in the "true positive" group, the LR model predicted an 80.0% probability of EC (Fig. 6G). For another patient in the "true negative" group, the decision leaned toward "EC" with a probability of 3.0% (Supplementary Fig. 6, Supplemental Digital Content 1, http://links.lww.com/MENO/B463). Besides, a force plot of interpretation for patients in the original cohort was illustrated in Supplementary Figure 7, Supplemental Digital Content 1, http://links.lww.com/MENO/B463. The *x*-axis represented each individual, and the *y*-axis represented the contributions of the features. An increased red part for each patient represented a greater probability toward the decision of "EC."

Establishment of predictive nomogram

Meanwhile, a nomogram incorporating these independent parameters was constructed to visualize the model (Fig. 7). Each parameter was assigned a score based on the characteristics of each individual, and the total score was then calculated to obtain the risk probability.[36] ROC analysis in the training set showed that the AUC of the nomogram model was 0.82 (95% CI, 0.76-0.88), with a sensitivity of 84%, a specificity of 67%, a PPV of 91%, and an NPV of 51% at the cutoff point of 0.207, suggesting the superior differential diagnostic performance of the model (Fig. 8A). In the internal validation cohort, the AUC was 0.82 (95% CI, 0.76-0.87), with 78% sensitivity, 68% specificity, 91% PPV, and 44% NPV (Fig. 8B). In the external

TABLE 5. Performance of machine learning models for predicting endometrial malignancy

Model	AUC	Sensitivity	Specificity	F1 score	Accuracy	PPV	NPV
DT	0.702	0.29	0.92	0.32	0.83	0.36	0.88
Gaussian	0.738	0.32	0.95	0.39	0.86	0.50	0.89
KNN	0.734	0.10	1.00	0.18	0.88	0.99	0.87
GBM	0.778	0.42	0.94	0.46	0.87	0.52	0.90
SVM	0.754	0.03	0.99	0.06	0.87	0.50	0.87
XGBoost	0.780	0.41	0.93	0.43	0.87	0.47	0.92
RF	0.800	0.32	0.97	0.42	0.89	0.60	0.91
LR	0.810	0.78	0.98	0.59	0.88	0.56	0.89
LightGBM	0.800	0.32	0.94	0.38	0.87	0.44	0.91

AUC, area under the curve; DT, decision tree; Gaussian, Gaussian naive Bayesian model; GBM, Gradient Boosting Model; KNN, K-Nearest Neighbors; LightGBM, light gradient boosting machine; LR, logistic regression; NPV, negative predictive value; PPV, positive predictive value; RF, random forest; SVM, support vector machine; XGBoost, eXtreme gradient boosting.

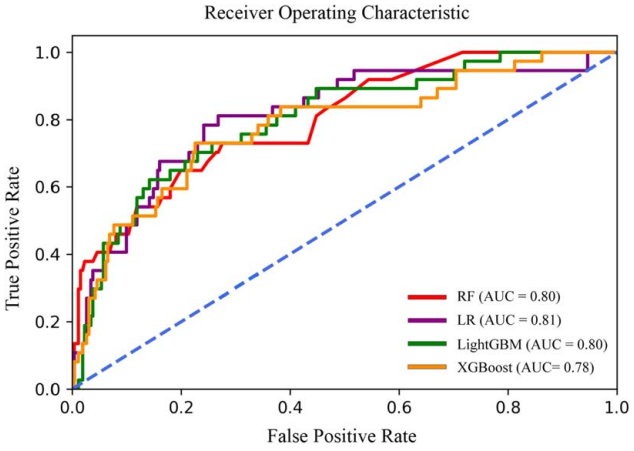

FIG. 5. Performance of ML models to predict EC. AUC, area under the receiver operating characteristic (ROC) curve; EC, endometrial carcinoma; LR, logistic regression; LightGBM, light gradient boosting machine; ML, machine learning; RF, random forest; XGboost, eXtreme gradient boosting.

validation cohort, which consisted of 226 eligible cases, the AUC reached 0.81 (95% CI, 0.72-0.88), with 82% sensitivity, 75% specificity, 96% PPV, and 35% NPV (Fig. 8C and Table 6). Detailed information on variables from the external validation set was provided in Supplementary Table 4, Supplemental Digital Content 1, http://links.lww.com/MENO/B463. The calibration plot indicated a high degree of consistency between the bias-corrected curve and the ideal curve in the training, internal validation set, and external validation sets, respectively (Fig. 8D–F). In addition, the clinical utility of the nomogram was evaluated via DCA. Results from the DCA demonstrated that this novel diagnostic nomogram provided greater benefit compared with two extreme strategies—treating all patients or treating none. Furthermore, the nomogram achieved optimal clinical applicability across nearly the entire range of threshold probabilities in the training set, internal validation set, and external validation set (Fig. 9A, B and C).

DISCUSSION

This was the first retrospective study with external cohort validation that aimed to investigate and compare nine ML models for the comprehensive predictive analysis of endometrial malignancy in postmenopausal patients presenting with asymptomatic endometrial thickening. We screened out a set of independent predictive risk factors and constructed a practical preoperative prediction nomogram model using clinically accessible data from the medical system, including clinical, ultrasonographic, and blood-related variables. Furthermore, our study provided pictorial and meaningful explanations using the SHAP method.

Current management of postmenopausal women regarding endometrial biopsy or hysteroscopy relies on clinical symptoms and ultrasound findings.[37] TVUS was an extremely common and noninvasive examination in gynecology, and an accumulating body of research indicated that ET measurement via TVUS was a vital factor in EC screening.[4,38] Women with postmenopausal abnormal bleeding and ET <5 mm as measured by TVUS were judged to have an NPV of 99% for EC and could refrain from endometrial sampling.[39,40] Sonographic ET ≥ 5 mm was supposed to be associated with a high risk of EC in women with PMB,[7] and then it was necessary to obtain an endometrial sample to exclude malignancy. In addition, more than 10%-15% of women with EC were asymptomatic at the time of diagnosis, and the incidence of endometrial malignancy among patients with asymptomatic polyps or thickened endometrium was very low.[41] The clinical management of this population had not been standardized. If the ET threshold of 4 or 5 mm for patients with vaginal bleeding was applied to asymptomatic women, the yield of invasive procedures (hysteroscopy and curettage) would cause unnecessary interventions and severe complications, traumatizing the physical and psychological well-being of the most elderly asymptomatic individuals.[42] To determine the optimal cutoff value of ET and establish a highly available model for this population, we retrospectively analyzed 745 postmenopausal patients with asymptomatic endometrial thickening, which was defined as postmenopausal double-layered ET ≥ 5 mm.[43,44] To avoid overfitting of data, the cohort was randomly separated into a training set and a validation set at a ratio of 7:3. Our analysis revealed that age, time of menopause, and other clinical conditions (systemic arterial hypertension, diabetes, and use of tamoxifen) were not recognized as risk factors for endometrial malignancy. Similarly, Jokubkiene et al[45] reported that among asymptomatic postmenopausal women, there were no substantial differences in ultrasound findings and pathological results between those who received hormone therapy and those who did not[45], which still requires extensive research to confirm.

Besides that, parity, Doppler flow signals, ET, CA125, and D-dimer were identified as independent risk factors for EC and precancerous lesions in postmenopausal patients. We put forward that endometrial lesions with positive Doppler flow signals could serve as an indicator of nonbenign endometrial pathology, which was in agreement with Li's statement.[46] In addition, we proposed that an ET of 8.15 mm was the optimal threshold to predict EC and precancerous lesions with 75% sensitivity and 68.0% specificity in the asymptomatic group. Consistently, Park et al[47] found that the ultrasonographic measurement of ET exhibited high diagnostic efficacy in predicting endometrial pathology, with an optimal cutoff value of 8 mm with a sensitivity of 100% and a specificity of 24.3% in premenopausal and postmenopausal women. Meanwhile, Ai et al[38] considered that the proper threshold of ET in predicting malignancy was 9.5 mm with 71.70% sensitivity and 71.69% specificity in asymptomatic women. Suarez et al[48] demonstrated that the ET threshold of 8 mm was statistically significant in asymptomatic postmenopausal women, and when the cutoff point was ≥ 12.55 mm, the possibility of endometrial malignancies increased by 4.68 times. Nevertheless, Goldstein[13] suggested that there was no association between Doppler flow or resistive index and the risk of

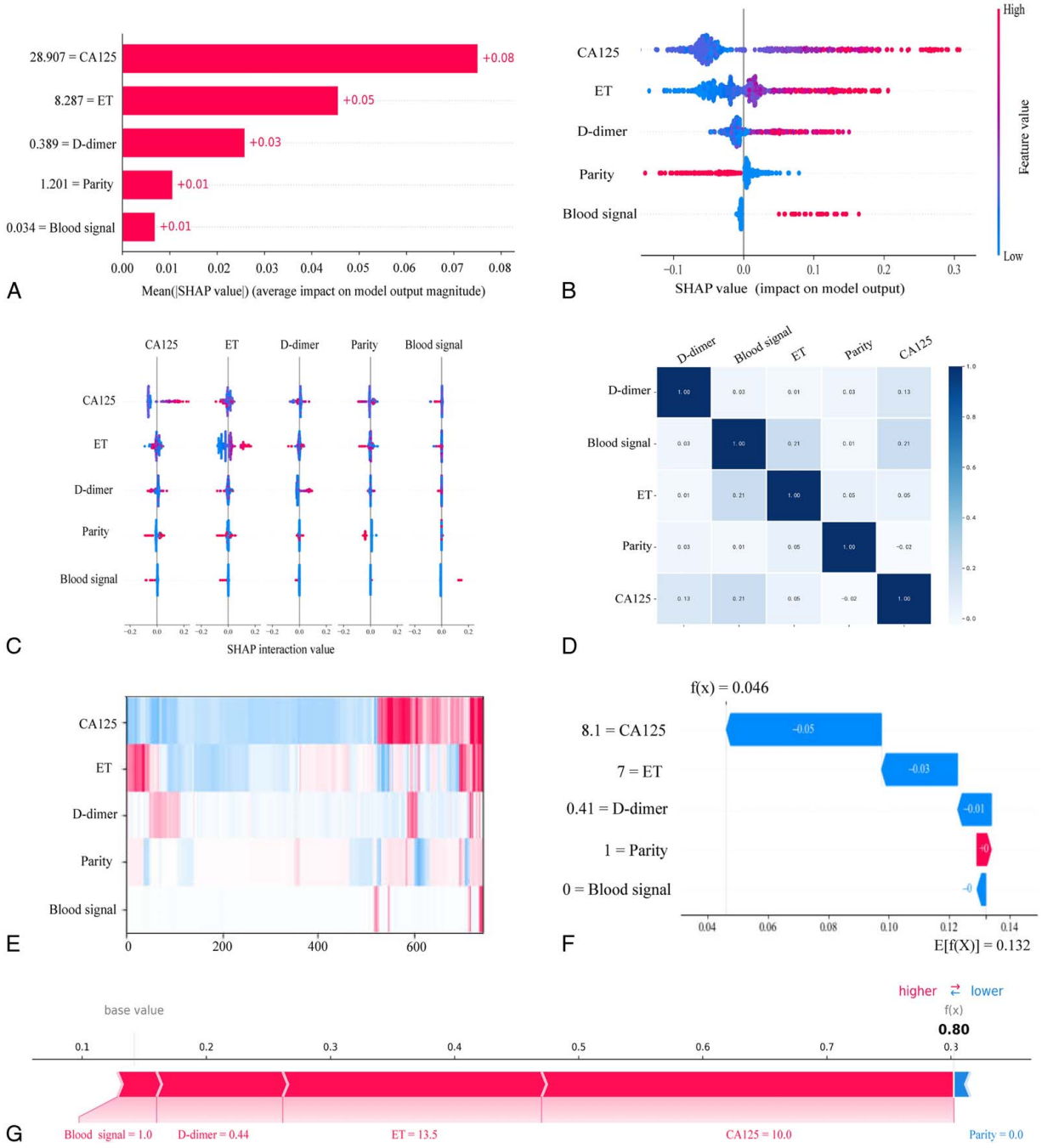

FIG. 6. Global model interpretation by the SHAP method. (**A**) The classified bar charts of the SHAP summary plots show the influence of each parameter on the model. (**B**) The beeswarm map of the model by SHAP shows the relationship between the characteristic value and the predicted probability through colors, including positive (red color) and negative (blue color) predictive effects. (**C, D**) SHAP interaction plots for the features affecting the prediction of endometrial malignancy. (**E**) SHAP absolute value heat map for all postmenopausal asymptomatic patients. The x-axis represented each instance, the feature importance was displayed in descending order on the *y*-axis, and the color described the direction and strength of the influence of the feature on the instance. (**F**) Waterfall plot of the risk contributed by each feature for the individual at low risk of developing EC. (**G**) Interpretability analysis of one independent sample by force plot. The SHAP value represented the predictive characteristics of individual patients and the contribution of each to the predictive malignancy. The number in bold was the probability forecast value ($f(x)$), while the base value was the predicted value without providing input to the model. The $f(x)$ was the logarithmic ratio of each observation. Red features indicated increased risk of malignancy, and blue features indicated reduced risk of malignancy. The length of the arrows helped visualize the extent to which the prediction was affected. The longer the arrow, the greater the effect. CA125, cancer antigen 125; EC, endometrial carcinoma; SHAP, SHapley Additive exPlanation.

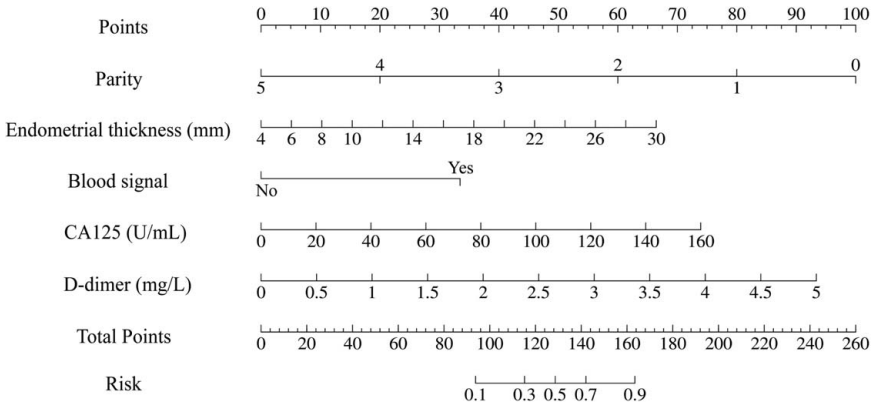

FIG. 7. A nomogram for predicting endometrial malignancy in postmenopausal asymptomatic patients. CA125, cancer antigen 125.

neoplasm in a study of 61 women with polyps. Karlsson et al[49] revealed that the utility of TVUS to exclude pathology should not be extrapolated to asymptomatic postmenopausal women without bleeding, and an endometrial measurement >4 mm does not need to routinely trigger evaluation. In addition, on the basis of survival measures, Segev et al[50] considered that screening for EC in symptomatic women had yet to be proven as an effective preventive measure; thus, invasive operations in asymptomatic women with incidental ultrasonographic findings should be carefully weighed. These distinct findings of scholars may result from imbalances in the baseline data, selection bias, and the limited sample size, and may not synchronously take clinical features, ultrasonic manifestations, and hematological tests into account, which offered guidance for our research.

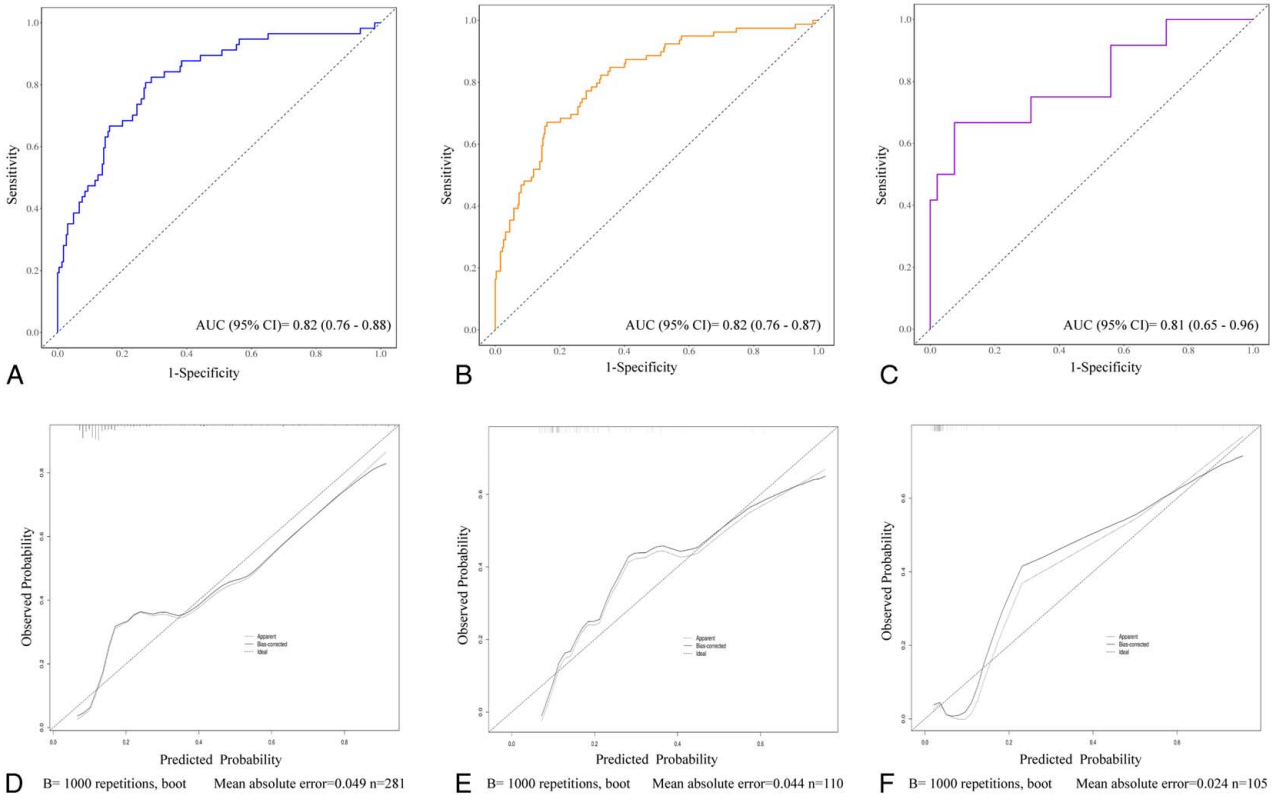

FIG. 8. ROC analyses and the calibration curves of the promising predictive model. ROC analysis in the training (**A**), internal validation data set (**B**), and external validation data set (**C**), respectively. The calibration curves of the training (**D**), internal validation data set (**E**), and external validation data set (**F**), respectively. AUC, area under the curve; ROC, receiver operating characteristic.

TABLE 6. The evaluation of the performance of the nomogram

Data set	AUC (95% CI)	Accuracy (95% CI)	Sensitivity (95% CI)	Specificity (95% CI)	PPV (95% CI)	NPV (95% CI)
Training set	0.82 (0.76-0.88)	0.80 (0.75-0.85)	0.84 (0.79-0.89)	0.67 (0.54-0.79)	0.91 (0.87-0.95)	0.51 (0.40-0.63)
Internal validation set	0.82 (0.76-0.87)	0.76 (0.67-0.84)	0.78 (0.70-0.87)	0.68 (0.49-0.88)	0.91 (0.84-0.97)	0.44 (0.27-0.61)
External validation set	0.81 (0.65-0.96)	0.81 (0.72-0.88)	0.82 (0.74-0.90)	0.75 (0.51-0.99)	0.96 (0.92-1.00)	0.35 (0.16-0.53)

AUC, area under the curve; NPV, negative predictive value; PPV, positive predictive value.

Hence, unlike the majority of current research that depended on a single ET indicator, our work focused on establishing a comprehensive preoperative nomogram model by integrating five independent risk factors—including parity, Doppler flow signals, ET, CA125, and D-dimer—via multivariate regression analysis. The nomogram was concise and intuitive for clinical use. Most importantly, it was validated in both the internal and external validation cohorts, with corresponding AUC values of 0.82 (95% CI, 0.76-0.87) and 0.81 (95% CI, 0.72-0.88), respectively. Both the internal and external calibration curves indicated a close match between the observed and predicted probabilities. The DCA curves revealed superior net benefits across a threshold probability range (15%-95%) compared with that of treat-all-patients or treat-none-patients, which highlighted the excellent performance of the model.

To date, there have been few in-depth investigations into EC prediction in asymptomatic postmenopausal women. This was primarily due to the small number of malignant cases and the heterogeneous underlying pathophysiology of EC, which has led to biased conclusions and limited clinical utility. In the present study, we systematically collected 97 premalignant and malignant cases over the past 7 years. This approach increased the proportion of malignant cases, thereby enhancing the credibility and relevance of our analysis. The ML technique was a powerful computational method for handling complex and extensive data, as it could process highly variable data sets and capture the complex relationships between variables in a flexible manner.[51] Combining readily available clinical data with sophisticated ML algorithms could facilitate the development of clinical prediction models, making them more accessible and useful for clinicians and researchers.[52] Among nine ML models, the LR model yielded the optimal AUC value, along with a strong net benefit and applicability across a high threshold probability range. In line with our findings, Lei et al[28] also proved that the LR method had unexceptionable predictive value in the field of medicine. Although additional variables may provide more information for the prediction model, including too many features could restrict the model's clinical applicability, and incorporating non-causal features may reduce prediction accuracy.[53] At present, we employed an intersection approach combining multivariate regression analysis and LASSO to screen 5 independent factors from 41 variables for model construction. This dual-method screening strategy reduced biases associated with single-method variable selection, thereby enhancing the credibility and robustness of the developed model. The features could be conveniently obtainable before routine surgery, making the model a promising tool for identifying endometrial malignancy in postmenopausal women with early endometrial thickening.

The ML technique had been characterized as a "black-box" without a direct explanation about how predictions were derived. This lack of transparency might cause clinicians to hesitate in using it, as they are reluctant to make medical decisions on opaque information.[54] This brought to light another advantage of our research, namely, we used the SHAP approach to interpret the "black-box." The SHAP method could offer two explanatory approaches: a global explanation, which illustrated the model's general functionality, and a local one, which explained how the model produced a specific prediction for an elderly patient by incorporating their unique data.[23,55] We assessed the contribution of each predictor

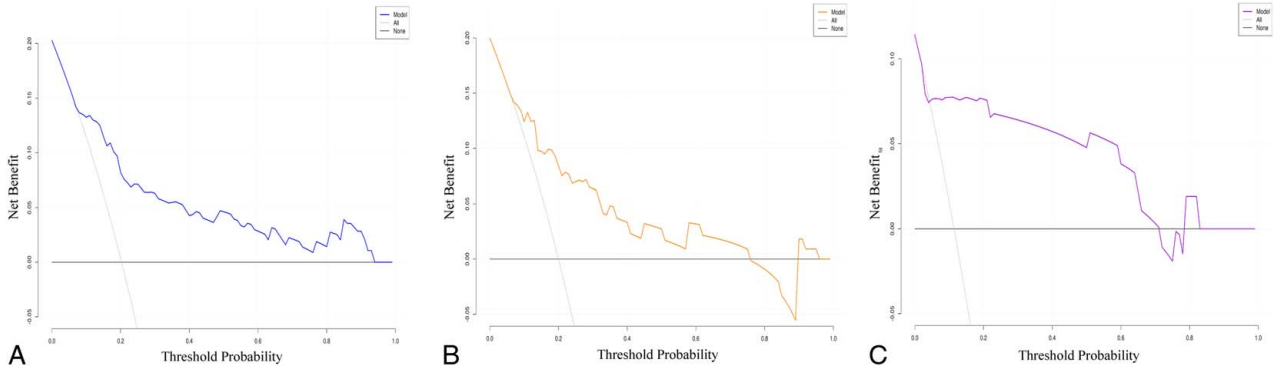

FIG. 9. Decision curve for evaluating the performance of the nomogram. DCA in the training cohort (**A**), internal validation cohort (**B**), and external validation cohort (**C**). DCA, decision curve analysis.

variable to the outcome predicted by the LR model. The concentration of CA125 had the strongest predictive value for all prediction horizons, followed by ET, D-dimer, parity, and Doppler flow signals. With SHAP force plots, the features associated with each individual patient and their respective contributions to malignancy prediction could be presented in a clear, intuitive manner.

When discussing the implications of our findings, it was essential to recognize several limitations inherent in the study. First, endometrial tumors presented with complex pathophysiological processes and were linked to a wide range of etiologies. The issue of whether this model performed well in predicting various EC subtypes remained an open question. Second, due to gaps in data availability and constraints of the information system, several hematological parameters (including liver and kidney function, blood lipids, calcium ions, and magnesium ions) and additional ultrasound indicators (such as uniform echogenicity, intracavitary fluid, and uterine cavity vascular patterns) were not incorporated into the analytical framework. There was a lack of nationwide data sources, and selection bias was present in the process of data input. Fortunately, robust cross-validation and external validation procedures provided sufficient statistical power to thoroughly investigate the prediction model in this study. Third, this model was developed based on the Chinese population, and its applicability to global populations had not yet been explored. Further investigation was required to evaluate its generalizability.

CONCLUSIONS

We successfully developed an explainable ML model for predicting endometrial precancerous and cancerous lesions in postmenopausal women with asymptomatic endometrial thickening. This model was constructed using clinical, ultrasound, and hematological data—all of which could be easily extracted from the medical information systems. In both internal and external validation cohorts, the final nomogram model exhibited remarkable accuracy in predicting endometrial malignancy. Owing to its broad clinical applicability, the model would be a promising tool for clinical decision-making, potentially preventing unnecessary invasive surgeries in most benign patients.

REFERENCES

1. Siegel RL, Miller KD, Wagle NS, Jemal A. Cancer statistics, 2023. *CA Cancer J Clin* 2023;73:17-48. doi:10.3322/caac.21763
2. Sung H, Siegel RL, Rosenberg PS, Jemal A. Emerging cancer trends among young adults in the USA: analysis of a population-based cancer registry. *Lancet Public Health* 2019;4:e137-e147. doi:10.1016/s2468-2667(18)30267-6
3. Clarke MA, Long BJ, Del Mar Morillo A, Arbyn M, Bakkum-Gamez JN, Wentzensen N. Association of endometrial cancer risk with postmenopausal bleeding in women: a systematic review and meta-analysis. *JAMA Intern Med* 2018;178:1210-1222. doi:10.1001/jamainternmed.2018.2820
4. Committee on Practice Bulletins—Gynecology and the Society of Gynecologic Oncology's Clinical Practice Committee. Practice bulletin no. 149: Endometrial cancer. *Obstet Gynecol* 2015;125:1006-1026. doi:10.1097/01.AOG.0000462977.61229.de
5. Palipana D, Fomin I, Russell E, et al. Investigating women with postmenopausal bleeding: the utility of endometrial thickness in transvaginal ultrasound. *Aust NZ J Obstet Gynaecol* 2020;60:773-775. doi:10.1111/ajo.13183
6. Saccardi C, Spagnol G, Bonaldo G, Marchetti M, Tozzi R, Noventa M. New light on endometrial thickness as a risk factor of cancer: what do clinicians need to know? *Cancer Manag Res* 2022;14:1331-1340. doi:10.2147/cmar.s294074
7. Smith-Bindman R, Weiss E, Feldstein V. How thick is too thick? When endometrial thickness should prompt biopsy in postmenopausal women without vaginal bleeding. *Ultrasound Obstet Gynecol* 2004;24:558-565. doi:10.1002/uog.1704
8. Vitale SG, Riemma G, Haimovich S, et al. Risk of endometrial cancer in asymptomatic postmenopausal women in relation to ultrasonographic endometrial thickness: systematic review and diagnostic test accuracy meta-analysis. *Am J Obstet Gynecol* 2023;228:22-35.e22. doi:10.1016/j.ajog.2022.07.043
9. Giannella L, Mfuta K, Setti T, Boselli F, Bergamini E, Cerami LB. Diagnostic accuracy of endometrial thickness for the detection of intrauterine pathologies and appropriateness of performed hysteroscopies among asymptomatic postmenopausal women. *Eur J Obstet Gynaecol Reprod Biol* 2014;177:29-33. doi:10.1016/j.ejogrb.2014.03.025
10. Quaranta M, Maillou K, D'Souza N, Pathiraja P. Incidental finding of thickened endometrium in postmenopausal women: a survey of endometrial cancer. *Cureus* 2023;15:e38538. doi:10.7759/cureus.38538
11. Louie M, Canavan TP, Mansuria S. Threshold for endometrial sampling among postmenopausal patients without vaginal bleeding. *Int J Gynaecol Obstet* 2016;132:314-317. doi:10.1016/j.ijgo.2015.07.023
12. Famuyide AO, Breitkopf DM, Hopkins MR, Laughlin-Tommaso SK. Asymptomatic thickened endometrium in postmenopausal women: malignancy risk. *J Minim Invasive Gynecol* 2014;21:782-786. doi:10.1016/j.jmig.2014.03.004
13. Goldstein SR. Modern evaluation of the endometrium. *Obstet Gynecol* 2010;116:168-176. doi:10.1097/AOG.0b013e3181dfd557
14. Garbi M. National Institute for Health and Care Excellence clinical guidelines development principles and processes. *Heart* 2021;107:949-953. doi:10.1136/heartjnl-2020-318661
15. Wang J, Peng X, Xia E, et al. When is it necessary to perform biopsy in asymptomatic postmenopausal women with incidental finding of thickened endometrium? *Eur J Obstet Gynaecol Reprod Biol* 2024;302:104-110. doi:10.1016/j.ejogrb.2024.08.016
16. Temur I, Kucukgoz Gulec U, Paydas S, Guzel AB, Sucu M, Vardar MA. Prognostic value of pre-operative neutrophil/lymphocyte ratio, monocyte count, mean platelet volume, and platelet/lymphocyte ratio in endometrial cancer. *Eur J Obstet Gynaecol Reprod Biol* 2018;226:25-29. doi:10.1016/j.ejogrb.2018.05.028
17. Li J, Jiang R, Liu WS, et al. A large cohort study reveals the association of elevated peripheral blood lymphocyte-to-monocyte ratio with favorable prognosis in nasopharyngeal carcinoma. *PLoS ONE* 2013;8:e83069. doi:10.1371/journal.pone.0083069
18. Templeton AJ, Ace O, McNamara MG, et al. Prognostic role of platelet to lymphocyte ratio in solid tumors: a systematic review and meta-analysis. *Cancer Epidemiol Biomarker Prev* 2014;23:1204-1212. doi:10.1158/1055-9965.epi-14-0146
19. Templeton AJ, McNamara MG, Šeruga B, et al. Prognostic role of neutrophil-to-lymphocyte ratio in solid tumors: a systematic review and meta-analysis. *J Natl Cancer Inst* 2014;106:dju124. doi:10.1093/jnci/dju124
20. Guo Y, Jiang T, Ouyang L, et al. A novel diagnostic nomogram based on serological and ultrasound findings for preoperative prediction of malignancy in patients with ovarian masses. *Gynecol Oncol* 2021;160:704-712. doi:10.1016/j.ygyno.2020.12.006
21. Han Y, Park IS, Kim SI, et al. Increasing serum gamma-glutamyltransferase level accompanies a rapid increase in the incidence of endometrial cancer in Korea: a nationwide cohort study. *Gynecol Oncol* 2021;161:864-870. doi:10.1016/j.ygyno.2021.03.024
22. Balachandran VP, Gonen M, Smith JJ, DeMatteo RP. Nomograms in oncology: more than meets the eye. *Lancet Oncol* 2015;16:e173-e180. doi:10.1016/s1470-2045(14)71116-7
23. Li J, Liu S, Hu Y, Zhu L, Mao Y, Liu J. Predicting mortality in

intensive care unit patients with heart failure using an interpretable machine learning model: retrospective cohort study. *J Med Internet Res* 2022;24:e38082. doi:10.2196/38082
24. Hsu WH, Ko AT, Weng CS, et al. Explainable machine learning model for predicting skeletal muscle loss during surgery and adjuvant chemotherapy in ovarian cancer. *J Cachexia Sarcopenia Muscle* 2023;14:2044-2053. doi:10.1002/jcsm.13282
25. Shi H, Yang D, Tang K, et al. Explainable machine learning model for predicting the occurrence of postoperative malnutrition in children with congenital heart disease. *Clin Nutr* 2022;41:202-210. doi:10.1016/j.clnu.2021.11.006
26. Timmerman D, Valentin L, Bourne TH, Collins WP, Verrelst H, Vergote I. Terms, definitions and measurements to describe the sonographic features of adnexal tumors: a consensus opinion from the International Ovarian Tumor Analysis (IOTA) Group. *Ultrasound Obstet Gynecol* 2000;16:500-505. doi:10.1046/j.1469-0705.2000.00287.x
27. Kong W, Pei Z, Guo Z, Ran X, Zhao J. Relationship matters: using machine learning methods to predict the mental health severity of Chinese college freshmen during the pandemic period. *J Affect Disord* 2025;369:392-403. doi:10.1016/j.jad.2024.09.168
28. Lei T, Guo J, Wang P, et al. Establishment and validation of predictive model of tophus in gout patients. *J Clin Med* 2023;12:1755. doi:10.3390/jcm12051755
29. Yang F, Li C, Yang W, et al. Development and validation of an explainable machine learning model for predicting multidimensional frailty in hospitalized patients with cirrhosis. *Brief Bioinform* 2024;25:bbae491. doi:10.1093/bib/bbae491
30. Hu J, Xu J, Li M, et al. Identification and validation of an explainable prediction model of acute kidney injury with prognostic implications in critically ill children: a prospective multicenter cohort study. *EClinicalMedicine* 2024;68:102409. doi:10.1016/j.eclinm.2023.102409
31. Zhang X, Wang C, Zheng D, et al. Radiomics nomogram based on multi-parametric magnetic resonance imaging for predicting early recurrence in small hepatocellular carcinoma after radiofrequency ablation. *Front Oncol* 2022;12:1013770. doi:10.3389/fonc.2022.1013770
32. Cong R, Kong F, Ma J, Li Q, Wu Q, Ma X. Combination of preoperative neutrophil-lymphocyte ratio, platelet-lymphocyte ratio and monocyte-lymphocyte ratio: a superior prognostic factor of endometrial cancer. *BMC Cancer* 2020;20:464. doi:10.1186/s12885-020-06953-8
33. Cummings M, Merone L, Keeble C, et al. Preoperative neutrophil: lymphocyte and platelet:lymphocyte ratios predict endometrial cancer survival. *Br J Cancer* 2015;113:311-320. doi:10.1038/bjc.2015.200
34. Sauerbrei W, Royston P, Binder H. Selection of important variables and determination of functional form for continuous predictors in multivariable model building. *Stat Med* 2007;26:5512-5528. doi:10.1002/sim.3148
35. Pourhoseingholi MA, Baghestani AR, Vahedi M. How to control confounding effects by statistical analysis. *Gastroenterol Hepatol Bed Bench* 2012;5:79-83.
36. Yu Y, Li Y, Yang X, Fan Q, Cao D, Wang Y. Daily variations and levels of human chorionic gonadotropin before methotrexate treatment as predictors of treatment success. *J Obstet Gynaecol Res* 2022;48:3128-3136. doi:10.1111/jog.15413
37. Wang J, Gao S, Wang J, Wang T. A risk prediction nomogram of endometrial carcinoma and precancerous lesions in postmenopausal women: a retrospective study. *Medicine (Baltimore)* 2023;102:e33087. doi:10.1097/md.0000000000033087
38. Ai F, Wang Y, Zhou L, Wang S. Clinicopathologic characteristics and risk factors for endometrial malignancy in postmenopausal women with endometrial thickening. *Menopause* 2022;29:137-143. doi:10.1097/GME.0000000000001903
39. Gull B, Carlsson S, Karlsson B, Ylöstalo P, Milsom I, Granberg S. Transvaginal ultrasonography of the endometrium in women with postmenopausal bleeding: is it always necessary to perform an endometrial biopsy? *Am J Obstet Gynecol* 2000;182:509-515. doi:10.1067/mob.2000.103092
40. Alcázar JL, Bonilla L, Marucco J, et al. Risk of endometrial cancer and endometrial hyperplasia with atypia in asymptomatic postmenopausal women with endometrial thickness ≥11 mm: a systematic review and meta-analysis. *J Clin Ultrasound* 2018;46:565-570. doi:10.1002/jcu.22631
41. Elfayomy AK, Soliman BS. Risk factors associated with the malignant changes of symptomatic and asymptomatic endometrial polyps in premenopausal women. *J Obstet Gynaecol India* 2015;65:186-192. doi:10.1007/s13224-014-0576-6
42. Segev Y, Dain-Sagi L, Lavie O, Sagi S, Gemer O. Is there a survival advantage in diagnosing endometrial cancer in asymptomatic patients? A systemic review and meta-analysis. *J Obstet Gynaecol Canada: JOGC = Journal d'obstetrique et gynecologie du Canada: JOGC* 2020;42:481-487.e482. doi:10.1016/j.jogc.2019.04.020
43. Rotenberg O, Goldberg GL. The significance of "atrophic endometrium" in women with postmenopausal bleeding. *Arch Gynecol Obstet* 2022;306:579-583. doi:10.1007/s00404-022-06540-1
44. Yao L, Li C, Cheng J. The relationship between endometrial thickening and endometrial lesions in postmenopausal women. *Arch Gynecol Obstet* 2022;306:2047-2054. doi:10.1007/s00404-022-06734-7
45. Jokubkiene L, Sladkevicius P, Valentin L. Transvaginal ultrasound examination of the endometrium in postmenopausal women without vaginal bleeding. *Ultrasound Obstet Gynecol* 2016;48:390-396. doi:10.1002/uog.15841
46. Li Z, Li L. Risk of malignancies among asymptomatic postmenopausal women with thickened endometrium: a cohort study. *Medicine (Baltimore)* 2019;98:e14464. doi:10.1097/MD.0000000000014464
47. Park YR, Lee SW, Kim Y, Bae IY, Kim YM. Endometrial thickness cut-off value by transvaginal ultrasonography for screening of endometrial pathology in premenopausal and postmenopausal women. *Obstet Gynecol Sci* 2019;62:445. doi:10.5468/ogs.2019.62.6.445
48. Suarez MB, Benetti-Pinto CL, Gibran L, Yela Daniela A. Asymptomatic postmenopausal women: what are the risk factors for endometrial malignancies? A multicentric retrospective study. *Gynecol Endocrinol* 2021;37:853-856. doi:10.1080/09513590.2020.1843621
49. Karlsson B, Granberg S, Wikland M, Ylöstalo P, Valentin L. Transvaginal ultrasonography of the endometrium in women with postmenopausal bleeding—a Nordic multicenter study. *Am J Obstet Gynecol* 1995;172:1488-1494. doi:10.1016/0002-9378(95)90483-2
50. Segev Y, Dain-Sagi L, Lavie O, Sagi S, Gemer O. Is there a survival advantage in diagnosing endometrial cancer in asymptomatic patients? A systematic review and meta-analysis. *J Obstet Gynaecol Canada* 2020;42:481-487. doi:10.1016/j.jogc.2019.04.020
51. Liu X, Wang Y, Wang Y, et al. A machine learning-based nomogram model for predicting the recurrence of cystitis glandularis. *Ther Adv Urol* 2024;16:17562872241290183. doi:10.1177/17562872241290183
52. Goecks J, Jalili V, Heiser LM, Gray JW. How machine learning will transform biomedicine. *Cell* 2020;181:92-101. doi:10.1016/j.cell.2020.03.022
53. Li Y, Sperrin M, Ashcroft DM, van Staa TP. Consistency of variety of machine learning and statistical models in predicting clinical risks of individual patients: longitudinal cohort study using cardiovascular disease as exemplar. *BMJ (Clinical research ed)* 2020;371:m3919. doi:10.1136/bmj.m3919
54. Chung H, Ko Y, Lee IS, et al. Prognostic artificial intelligence model to predict 5 year survival at 1 year after gastric cancer surgery based on nutrition and body morphometry. *J Cachexia Sarcopenia Muscle* 2023;14:847-859. doi:10.1002/jcsm.13176
55. Liu C, Zhang K, Yang X, et al. Development and validation of an explainable machine learning model for predicting myocardial injury after noncardiac surgery in two centers in China: retrospective study. *JMIR aging* 2024;7:e54872. doi:10.2196/54872

